International Journal of the Korean Society of Precision Engineering Vol. 4, No. 2, March 2003.

An Adaptive and Robust Controller for the Undersea Robot Manipulator

Young-Sik Kim[1] and Hyeung-Sik Choi[1]

[1] Division of Mechanical and Information Engineering Korea Maritime University, Pusan, South Korea

ABSTRACT

To coordinate the robot manipulator along the desired trajectory, the exact model of the dynamics is required. The added mass and added moment of inertia, buoyancy, drag force, and friction mainly affect the dynamics of the undersea robot manipulator, and they are quite complex and unknown. In this reason, the exact model of the undersea robot manipulator is difficult to obtain.

In this paper, instead of having efforts to get the exact model of the robot dynamics, a control-based approach was performed. We modeled the dynamics of the undersea robot manipulator whose parameters are unknown, and then applied a proposed direct adaptive and robust control, which is different from previous studies. The unknown added mass, and added moment of inertia, drag force and friction are estimated by the direct adaptive control scheme, and the drag force which is dominant disturbance is compensated by the robust control. Also, stability of the proposed control scheme is analyzed.

Key words : Adaptive Control, Robust control, Added mass, Added moment of inertia

1. Introduction

Remotely operated underwater vehicles (ROVs) and autonomous underwater vehicles (AUVs) are widely used in the marine research, offshore oil industry, and other applications. The dynamics of the industrial robot manipulator has been studied in many ways, but not the robot manipulator working under the sea. Under the sea, due to effects of the added mass, added moment of inertia, buoyancy, drag force, and static and Coulomb friction on the joints, its dynamic characteristics are quite different. Since these effects are very complex and highly nonlinear, it is not easy to achieve the exact model of the robot manipulator.

Not many research papers were presented on the undersea robot manipulator. One of them presented the modeling of a specific three DOF underwater robot manipulator was modeled and studied, but disturbances such as sea flow, waves, and currents were not considered[1]. In another paper, the dynamics of the manipulator are studied to control the underwater robot manipulator, but the drag force was the only parameter taken into consideration[2]. As a mobile base of underwater manipulators, an underwater robotic vehicle including manipulators was studied[3], where methods which measure open-loop dynamics from the trials performance of a prototype ROV was proposed. As a simulation approach, an optimal trajectory of the robotic vehicle was planned for the purpose of energy minimization[4], where a function space conjugate gradient method and a control vector parametrization method were applied.

Control strategies have been introduced to coordinate underwater robotic manipulators and vehicles. A robust trajectory control scheme was used for underwater vehicles where a sliding mode control algorithm was applied to coordinate the motion of the AUV[6], and a nonlinear robust feedback control was studied where compensating the coupling effects from the arm to the base of the underwater vehicle/manipulator system[7]. A discrete-time indirect

adaptive control algorithm was applied to control remotely operated underwater vehicles with adaptive method5. The robustness of the control system with respect to the nonlinear dynamic behavior and parameter uncertainties was investigated. Under the sea, currents and wave affect the dynamics of the manipulator, which were neglected in the previous papers.

In this paper, to reduce the effort of obtaining the exact model of the undersea robot manipulator and of controlling the undersea robot manipulator, a direct adaptive control scheme is proposed, which can estimate unknown parameters such as the added mass, added moment of inertia, frictional force, and drag force including currents and wave effects. In addition to this, a robust control scheme is devised to compensate for the drag force which is dominant disturbance to the robot. A stability analysis on the devised control scheme is shown based on Lyapunov theorem. A numerical simulation is given.

2. Dynamical Model of The Robot Manipulator

The n degree-of-freedom robot manipulator composed of rigid bodies is expressed based on Newton's and Euler's equations[8-9] as follows:

$$f_{i-1,i}-f_{i,i+1}-m_i\dot{v}_{ci}+m_ig=0,\ i=1,..,n \tag{1}$$

$$N_{i-1,i}-N_{i,i+1}+r_{i,ci}\times f_{i,i+1}-r_{i-1,ci}\times f_{i-1,i} -I_i\dot{\omega}_i-\omega_i\times(I_i\omega_i)=0,\ i=1...,n \tag{2}$$

where $f_{i-1,i}$ and $-f_{i,i+1}$ are the coupling forces applied to link i by link $i-1$ and $i+1$, respectively, m_i is the mass of link i; g is the acceleration of gravity, v_{ci} is the velocity of the centroid of link i with respect to the base coordinate frame, ω_i is the angular velocity vector; I_i is the centroidal inertia tensor of link i.

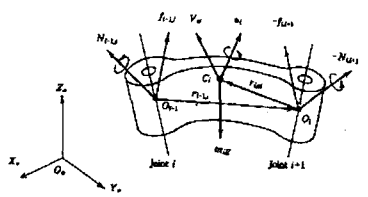

Fig. 1 Free body diagram of link i

By evaluating (1) and (2) for all the robot links, i = 1,....,n, the dynamics of the n-link robot manipulator is expressed into the matrix equation as

$$H(q)\ddot{q}+C(q,\dot{q})\dot{q}+G(q)=\tau \tag{3}$$

where $q\in R^{n\times1}$ is the joint angle vector, $\tau\in R^{n\times1}$ is the joint torque vector, $H(q)\in R^{n\times n}$ is the inertia matrix, $C(q,\dot{q})\in R^{n\times1}$ is the nonlinear force vector including the centripetal and Coriolis forces.

3. Dynamic Model of The Robot Manipulator under The Sea

Under the sea, the dynamics of the robot manipulator are quite different from ordinary ones due to several factors such as buoyancy, added mass, added moment of inertia[10], frictional force, drag force, and accelerated waves. The gravity acting on the manipulator is reduced by buoyancy as

$$m_i^o g=(m_i-\rho_s V_i)g \tag{4}$$

where ρ_s is the density of the sea water.

When the robot manipulator is accelerated, the fluid surrounding the links of the manipulator is accelerated, which is called the added mass and added moment of inertia. In this reason, actual mass and moment of inertia to be actuated are composed of the added mass and moment of inertia and original ones. The mass m^* and moment of inertia I^* which should be considered in the dynamics of undersea robot manipulator are expressed by the relation between the actual mass m_i, actual moment of inertia I_i and the added mass m_i', added moment of inertia I_i' of the ith link, respectively, as

$$m_i^*=m_i+m_i',\quad I_i^*=I_i+I_i' \tag{5}$$

where $m_i' = C_A \rho_s A_i l_i$, C_A is the coefficient of the added mass, A_i is the projected area of the ith link to the vertical plane of the accelerated direction of the ith link, l_i is the length of the ith link. The velocity distribution of the robot links is not linear due to the nonlinear manipulator dynamics and due to the nonlinear waves and currents so that A_i is difficult to calculate. The added moment of inertia is caused by the displaced fluid when the ith robot link is rotated around the centroid, which is complicate to model. The added mass and added moment of inertia are incorporated in (1) and (2) such that the Newton's and Euler's equations become

$$f_{i-1,i} - f_{i,i+1} - m_i^* \dot{v}_{ci} + m_i g = 0, \; i = 1, \ldots, n \tag{6}$$

$$N_{i-1,i} - N_{i,i+1} + r_{i,ci} \times f_{i,i+1} - r_{i-1,ci} \times f_{i-1,i} - I_i^* \dot{\omega}_i - \omega_i \times (I_i^* \omega_i) = 0, \; i = 1, \ldots, n \tag{7}$$

To have closed-form dynamic equations (6) and (7), the joint torque $\tau_i = N_{i-1,i}$ should be expressed explicitly by iterating equations (6) and (7) for $i = 1, \ldots, n$ In this way the closed-form dynamic equation of the n degree-of-freedom manipulator is given in a matrix form.

Due to sealing, the frictional force $F(q, \dot{q}) \in R^{n \times 1}$ representing the static and Coulomb friction force is not neglectable and is expressed as

$$F(q, \dot{q}) = c \; sgn(\dot{q}) + v\dot{q} \tag{8}$$

where $c \; sgn(\dot{q})$, $v\dot{q} \in R^{n \times 1}$ are Coulomb and viscous friction vector, c and v are Coulomb and viscous friction coefficients, respectively.

Besides those parameters, there exists drag force disturbing the robot dynamics, which is caused by the motion of the manipulator itself, waves and currents referred to reference[11], and are expressed as

$$\begin{cases} u = \xi_a v_w k \dfrac{\cosh k(-z+h)}{\sinh kh} \cos k(x - v_w t) \\ w = \xi_a v_w k \dfrac{\cosh k(-z+h)}{\sinh kh} \sin k(x - v_w t) \end{cases} \tag{9}$$

where u and w are the horizontal and vertical wave velocities. ξ_a is the wave amplitude, $k = \dfrac{2\pi}{L_w}$, L_w is the wave length i.e. the distance between one crest to the next. The ordinate for z is positive in the downward direction. The water depth h is a positive quantity. v_w is defined as

for shallow water ($h < L_w/20$): $v_w = \sqrt{gh}$,

for deep water ($h > L_w/20$): $v_w = (gL_w/2\pi)^{1/2}$.

The velocity vector of the waves is expressed as $u_w^T = [u^T \; w^T]$. The velocity of the currents u_c also affects the drag force. The relative velocity of the manipulators v_{ri} to the fluids around them is composed of the velocity of the manipulator u_{mi}, that of waves u_{vi}, and that of currents u_{ci} so that it is expressed as

$$v_{ri} = u_{mi} - u_{vi} - u_{ci} \tag{10}$$

which affects the dynamics of the manipulators as a drag force. The drag force exerting on the ith link by is expressed as

$$D_{fi} = -C_D (1/2) \rho v_{ri} \mid v_{ri} \mid A_i' \tag{11}$$

where A_i' is the projected area of the ith link to the vertical direction of v_{ri}. The drag force coefficient C_D varies according to the Reynolds number and the roughness of the robot links. The value of C_D is obtained from the experimental value in reference[9]. The drag force is expressed by Euler equation as

$$D_{di}-D_{di+1}+r_{i,a}\times D_{fi+1}-r_{i-1,a}\times D_{fi}=0, i=1,..,n \quad (12)$$

Iterating equation (12) for $i=1,....,n$ yields the torque applied on each link. Including all the equations (4,7,8,12) and expressing them into the closed-form matrix equation yield

$$H^*(q)\ddot{q}+C^*(q,\dot{q})\dot{q}+G^*(q)+F(q,\dot{q})+D=\tau \quad (13)$$

where $H^*(q)\in R^{n\times n}$ is the inertia matrix composed of the mass and moment of inertia including the added mass and moment of inertia for the links, $C^*(q,\dot{q})\in R^{n\times 1}$ is the Coriolis and centrifugal force, and nonlinear force, $G(q)^*\in R^{n\times 1}$ is the gravity force including buoyancy, $D\in R^{n\times 1}$ is the torque vector by the drag force.

4. Design of an Adaptive and Robust Controller

4.1 Design of an Adaptive Controller

In this paper, an adaptive controller is devised to estimate the uncertain parameters. A computed torque based controller is designed as

$$\tau=\widehat{H}^*(q)\ddot{u}_r+\widehat{C}^*(q,\dot{q})\dot{q}+G^*(q)+\widehat{F}(q,\dot{q})+\widehat{D}-K_DS \quad (14)$$

where

$\dot{u}_r=\dot{q}_d-K\dot{e}$, $\ddot{u}_r=\ddot{q}_d-K\dot{e}$,

$s=\dot{e}+Ke$, $e=q-q_d$,

and $\widehat{H}^*(q)$, $\widehat{C}^*(q,\dot{q})\in R^{n\times n}$ are estimates of $H^*(q)$ and $C^*(q,\dot{q})$, $\widehat{F}(q,\dot{q})$, $\widehat{D}\in R^{n\times 1}$ are estimates of $F(q,\dot{q})$ and D, $q_d\in R^{n\times 1}$ is a desired joint angle vector, the controller gains K_D, $K\in R^{n\times n}$ are diagonal positive matrices. Applying the controller to (13) yields

$$H^*\ddot{q}+C^*\dot{q}+G^*+F+D=\widehat{H}^*\ddot{u}_r+\widehat{C}^*\dot{q}+G^*+\widehat{F}+\widehat{D}-K_DS \quad (15)$$

In (15), the exact measurement of the parameters is impossible so that estimates of them are obtained by the adaptive control scheme. Arranging (15) yields

$$H^*\dot{s}+K_DS=\widetilde{H}^*\ddot{u}_r+\widehat{C}^*\dot{q}-C^*\dot{q}+\widetilde{D}+\widetilde{F} \quad (16)$$

where

$$\widetilde{H}^*=\widehat{H}^*-H^*,\quad \widetilde{F}^*=\widehat{F}^*-F^*,\quad \widetilde{D}=\widehat{D}-D$$

Under the sea, the speed of the manipulator is not fast such that the effect of added mass and added moment of inertia are not big enough to change the structure of the positive definite matrix H^*. In (16), K_D is designed as positive definite matrices. The error terms of the right side of (16) are reduced by the adaptive control algorithm. The Lyapunov function is

$$V=\frac{1}{2}s^TH^*s+\tilde{a}^T\Gamma^{-1}\tilde{a} \quad (17)$$

where the energy function V is $V\geq 0$. $\tilde{a}\in R^{1\times m}$ is the linearized estimation error vector of the added mass, added moment of inertia, coefficients of frictional force, and coefficients of drag force, $\Gamma\in R^{n\times n}$ is the control gain matrix. $\dot{V}\leq 0$ should be satisfied for the stability of (17). Differentiating V with respective to time yields

$$\begin{aligned}\dot{V}&=s^T(H^*\dot{s}+\frac{1}{2}\dot{H}^*s)+\dot{\tilde{a}}^T\Gamma^{-1}\tilde{a}\\&=s^T(\widetilde{H}^*\ddot{u}_r+\widehat{C}^*\dot{q}-C^*\dot{q}+\widetilde{D}+\widetilde{F}\\&\quad -K_DS+\frac{1}{2}\dot{H}^*s)+\dot{\tilde{a}}^T\Gamma^{-1}\tilde{a}\end{aligned} \quad (18)$$

Arranging (18) yields

$$\begin{aligned}\dot{V}&=s^T(\widetilde{H}^*\ddot{u}_r+\widehat{C}^*(s+\dot{u}_r)-C^*(s+\dot{u}_r)\\&\quad +\widetilde{D}+\widetilde{F}-K_DS+\frac{1}{2}\dot{H}^*s)+\dot{\tilde{a}}^T\Gamma^{-1}\tilde{a}\end{aligned} \quad (19)$$

In the structure of the dynamics of the robot manipulator, the skew-symmetric relation exists as

$$s^T(\dot{H}-2C(q,\dot{q}))s=0, \forall s \in R^{n\times 1} \quad (20)$$

(19) is expressed by the relation in (20) as

$$\dot{V}=s^T(\widetilde{H}^*\ddot{u}_r+\widetilde{C}^*\dot{u}_r-(K_D-\widehat{C}^*-C_{ad}+\frac{1}{2}\dot{H}_{ad})s + \widetilde{D}+\widetilde{F})+\dot{\tilde{a}}^T\Gamma^{-1}\tilde{a} \quad (21)$$

where $\dot{H}_{ad}$, $C_{ad} \in R^{n\times n}$ are the matrices composed of the added mass and added moment of inertia of H and C, respectively, and they are $H_{ad}=H^*-H$, $C_{ad}=C^*-C$. In (18), drag force D is the function of the relative velocity of the robot manipulator to that of the waves and currents. If they do not affect the drag force so that $u_{ci}+u_{wi}\approx 0$, then the drag force becomes the function of only u_{mi}. Eq (21) can be reexpressed as the following equation

$$\widetilde{H}^*\ddot{u}_r+\widetilde{C}^*\dot{u}_r+\widetilde{D}+\widetilde{F}=W(q,\dot{q},q_d,\dot{q}_d,\ddot{q}_d)\tilde{a} \quad (22)$$

where the regressor vector $W(q,\dot{q},q_d,\dot{q}_d,\ddot{q}_d) \in R^{n\times m}$ is composed of measurable variables. The adaptive controller for (22) is composed as

$$\dot{\hat{a}}=-\Gamma W^T s \quad (23)$$

Applying (23) to (21) yields a concise equation as

$$\dot{V}=-s^T(K_D-\widehat{C}^*-C_{ad}+\frac{1}{2}\dot{H}_{ad})s \quad (24)$$

If K_D is designed as $\lambda_{KD} > \lambda_{DI}$, where λ_{KD} is the minimum eigenvalue of K_D, and λ_{DI} is the maximum eigenvalue of $-\widehat{C}^*-C_{ad}+\frac{1}{2}\dot{H}_{ad}$.

Then $\dot{V}\le 0$ is satisfied such that stability of the closed loop dynamic equation (22) is guaranteed.

4.2 The Design of a Robust Controller

If the waves and currents are strong such that they can not be neglected, the drag force due to these should be robustly controlled. To do this, the drag force should be divided in to two terms: D_{mi} due to the velocity of the manipulator itself v_{mi} and D_{wci} due to the waves and currents $v_{wxi}+v_{ci}$. The equation for this is

$$D_{fi}=D_{mi}+D_{wci} \quad (25)$$

where

$$D_{mi}=-C_D(1/2)\rho v_{mi}|v_{mi}|A_i,$$
$$D_{wci}=-C_D(1/2)\rho(2v_{mi}v_{wci}+v_{wci}^2)A_i$$

By Euler equation, D_{mi} and D_{wci} can be expressed as torque vectors $D_m(q,\dot{q})$ and D_{wc}. $D_m(q,\dot{q})$ is estimated by the adaptive control scheme, and D_{wc} is controlled by the robust controller. Hence, a controller for the robot manipulator is designed as

$$\tau=\bar{\tau}+R \quad (26)$$

where $\bar{\tau}$ is the same structure with the controller in (19). Applying (26) to (14) yields

$$\dot{V}=-s^T((K_D-\widehat{C}^*-C_{ad}+\frac{1}{2}\dot{H}_{ad})s+s^T(D_{wc}+R) \quad (27)$$

where a robust controller R is designed as follows

$$R=-\frac{s}{\|s\|+\varepsilon}\|D_{wc}\| \quad (28)$$

where $\|*\|$ means L_2 norm, and $\|D_{wc}\|$ is bounded disturbance. In (27),

$$s^T(D_{wc}+R) \leq \|s\|\,\|D_{wc}\| + s^T R = s^T\left(\frac{s}{\|s\|}\|D_{wc}\| + R\right) \quad (29)$$

Applying R to (29) yields the following inequality

$$s^T\left(\frac{s}{\|s\|}\|D_{wc}\| - \frac{s}{\|s\|+\varepsilon}\|D_{wc}\|\right) \leq \varepsilon\|D_{wc}\| \quad (30)$$

The equation in (27) is expressed using (30) as

$$V \leq -\lambda' s^T s + \varepsilon\|D_{wc}\| \quad (31)$$

where positive value λ' is obtained by designing the control gain λ_{KD} as $\lambda_{KD} > \lambda_{DI}$. The uniformly ultimate boundedness of (31) is proved by Corless[12]. The block diagram of the control structure is shown as

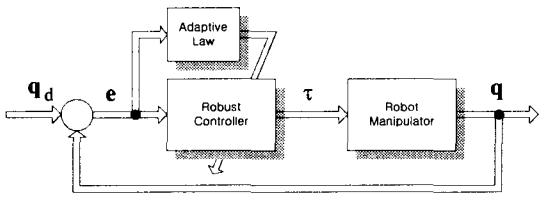

Fig. 2 Block diagram of the adaptive and robust controller

The parameters of the robust controller is updated by the adaptive law, and the robust control input τ in Eq. (26) is fed in a feedforward form, which is

$$\tau = \widehat{H}^*(q)\,\ddot{u}_r + \widehat{C}^*(q,\dot{q})\,\dot{q} + G^*(q) + \widehat{F}(q,\dot{q}) + \widehat{D} - K_D s + R$$

5. Simulation

For numerical simulation, the dynamics of the two axes planar arm is expressed as follows

$$H^*(q)\ddot{q} + C^*(q,\dot{q})\dot{q} + D = \tau \quad (32)$$

In simulation, the friction term is not considered to simply show the applicability of the proposed control algorithm, The matrix equation of (32) is as follows

$$\begin{bmatrix} h_{11} & h_{12} \\ h_{21} & h_{22} \end{bmatrix}\begin{bmatrix} \ddot{q}_1 \\ \ddot{q}_2 \end{bmatrix} + \begin{bmatrix} -c\dot{q}_2 & -c(\dot{q}_1+\dot{q}_2) \\ c\dot{q}_1 & 0 \end{bmatrix}\begin{bmatrix} \dot{q}_1 \\ \dot{q}_2 \end{bmatrix} + \begin{bmatrix} d_1 \\ d_2 \end{bmatrix} = \begin{bmatrix} \tau_1 \\ \tau_2 \end{bmatrix} \quad (33)$$

where

$$h_{11} = a_1 + 2a_3\cos(q_2)$$
$$h_{12} = h_{21} = a_2 + 2a_3\cos(q_2)$$
$$h_{22} = a_2,\quad c = a_3\sin(q_2)$$

$$a_1 = m_1^* L_{c1}^2 + m_2^*(L_1^2 + L_{c2}^2) + I_1^* + I_2^*$$
$$a_2 = m_2^* L_{c2}^2 + I_2^*,\quad a_3 = m_2^* L_1 L_{c2}$$

where the drag forces d_1 and d_2 applied to each link do not contain the effect of the waves and currents.

$$d_1 = -b_1 v_1|v_1|(L_{c1}) - b_2 v_2|v_2|(L_1 + L_{c2})$$
$$d_2 = -b_2 v_2|v_2|(L_{c2})$$

where v_1 and v_2 are the velocities of the centroid of link 1 and 2 in Cartesian coordinate, respectively, and b_1 and b_2 are as follows

$$b_1 = \frac{1}{2} C_d \rho A_1,\quad b_2 = \frac{1}{2} C_d \rho A_2$$

A controller for (33) is as follows

$$\tau = \widehat{H}^*(q)\,\ddot{u}_r + \widehat{C}^*(q,\dot{q})\,\dot{q} + \widehat{D}(q,\dot{q}) - K_D s + R \quad (34)$$

In (34), the drag force applied to each link does not contain the effect of the waves and currents. In (33), $a_1, a_2, a_3, b_1, b_2$are difficult to measure exactly such that an adaptive controller is applied to estimate the actual parameters. The estimation error vector is $\tilde{a} = [\tilde{a}_1\ \tilde{a}_2\ \tilde{a}_3\ \tilde{b}_1\ \tilde{b}_2]^T$ where $\tilde{a}_1 = \hat{a}_1 - a_1$ for

example. Also, the regressor W is 5×2 matrix composed of known parameters. The adaptive control algorithm is very useful in controling the uncertain undersea robot manipulator since it does not need exact modeling of the dynamics. In this simulation, the friction term is not considered, but it can be estimated in the same manner as other terms.

The surroundings of the robot manipulator is assumed as follows: the velocity of the current: v_c= 0.5(m/s);the wave length L_w=10(m), the wave amplitude ξ_a=0.5, and the depth of water h = 5(m). The operating position of the manipulator is at the bottom, z= -5(m); According to the definition, for v_w, deep water condition is selected such that v_w= $(gL_w/2\pi)^{1/2}$=3.949(m/sec). According to all the conditions, the maximum velocity of the sea water on the manipulator u_w $(w=0)$ is with $k=2\pi/L_w$ =0.628(rad/m) $u_w=v_{wa}=\xi_a v_w k\cosh k(-z+h)$= 0.107(m/s).

Using the given value of v_c and v_{wa}, $\|D_{wc}\|$ is decided such that the robust controller can be composed. The numerical data used to parameters of the two-link planar manipulator are in Table 1.

Table 1 Link parameters for numerical simulation

No.of Link	mass m1,m2 (kg)	moment of inertia I_1,I_2 (kg-m*m)	radius r_1,r_2 (m)	length L_1,L_2 (m)	centroid L_{c1},L_{c2} (m)
link 1	8	0.172	0.05	0.5	0.25
link 2	5	0.067	0.03	0.4	0.2

The shape of the links is circular cylinder. The inertia of the links is calculated based on I_1= (1/12) $m_1(3r_1^2+l_1^2)$ and I_2=(1/12) $m_2(r_2^2+l_2^2)$. The actual value of the added mass and added moment of inertia is assumed as

$$m_{ad1}=2(Kg),\ m_{ad2}=1.5\cos(q_2)(Kg),$$
$$I_{ad1}=0.1(Kg-m^2),\ I_{ad2}=0.04\cos(q_2)(Kg-m^2)$$

Since the projected areas of the robot links vary according to the direction of movement of the links, they are assumed as b_1= 1.17, b_2= 0.34cos(q_2).

The control gains are set as

$$K_D=\begin{bmatrix}50 & 0\\ 0 & 50\end{bmatrix},\quad K=\begin{bmatrix}10 & 0\\ 0 & 10\end{bmatrix},$$

γ_1=0.9, γ_2=0.2, γ_3=0.07,

γ_4=120, γ_5=0.5, ε=0.01

where γ_i is the diagonal component of 5×5 matrix.

Applying all the values of the parameters and gains to (34), the resulted plots are given in figures 3, 4, 5, 6, 7, and 8. These figures are the results of manipulator's trajectory tracking for three seconds and the results of the numerical simulation of closed loop dynamic equation (15) and the adaptive and robust control algorithm (23) and (26) using the Runge-Kutta 4th order integration scheme based on C language. The desired trajectories of the link 1 and 2 are π/6 (1-cos πt) and π/4 (1-cos πt), respectively. The velocities and accelerations are obtained by differentiating the trajectory function once and twice with respect to time.

In Figure 3, tracking errors between the desired and actual trajectory in Cartesian coordinate are shown. The dotted line represents the tracking errors when the control algorithm in (34) is applied without the adaptive and robust control algorithm. The solid line represents the tracking errors when the control algorithm in (34) is applied with adaptive control algorithm. In other words, the dotted line is the result without considering uncertain added mass, added moment of inertia, and drag force. Reversely, in the solid line, uncertain added mass, added moment of inertia, and drag force are adaptively controlled. The tracking errors with adaptive control are much less than the other ones. Figures 4, 5, 6 represent the estimation of a_1, a_2, a_3 which are concerned with the structure of the robot manipulator,

and Figures 7 and 8 represent the estimation of b_1, b_2 which are concerned with the drag force. The dotted lines represent the actual values including uncertain added mass and moment of inertia m_1^*, m_2^*, I_1^*, and I_2^* of robot links and the drag coefficients C_d and reflected areas A_1 and A_2. The solid lines represent the estimated values of the actual parameters. In figures 4~8, the actual values of parameters (dotted lines) varies since they are configuration dependent. In Fig. 3, a_1 contains uncertain parameters m_1^*, m_2^*, I_1^*, and I_2^*, which is compensated by the adaptive control law in Eq. (23). In Fig. 4 and 5, a_2 contains parameters m_2^* and I_2^*, and a_3 contains parameter m_2^*, which are compensated by the adaptive control law. In Figs 6 and 7, the drag terms b_1 and b_2 are identified. In b_2, the projected area A_2 varies according to the direction of movement of robot links which is function of $\cos(q_2)$. By the adaptive control law , they are compensated. In compensation action by the adaptive control law, the estimated values varies due to the variation of the actual values and the transient tracking errors. In the figures, the estimated values do not converge to the actual values of the parameters. The reason is that the actual values of the parameters are varying and the excitation of the tracking errors are not enough. The merit of the proposed direct adaptive control algorithm is that the tracking errors are reduced a lot or converge to zero even though the estimated parameter values do not converge to the actual ones. According to the results shown, though the exact estimation of the actual values of the unknown parameters is not achieved, good trajectory tracking is still achieved.

6. Conclusion

We modeled the undersea robot manipulator by considering the factors affecting the dynamics of the robot manipulator such as the added mass, added moment of inertia, drag, friction, and wave force. In control of the robot manipulator, the uncertain parameters are identified by the direct adaptive controller. To compensate for the effects of dominant disturbance, a robust control scheme is proposed. By the proposed control scheme, efforts to set up the exact model of the robot manipulator are reduced. According to the simulation results, though identification of parameters are not accurate, tracking errors are reduced significantly. In this reason, the proposed control scheme is appropriate for trajectory tracking of the uncertain undersea robot manipulator.

Acknowledgement

This research was supported by BK21 of Korea Maritime University

References

1. Kang, E. S., Song, J. S., Kim, J. H. and Cho, H. S., "Dynamic Characteristic and Control of Submerged Working Robot Manipulator," KSME, Vol. 5, No. 2, pp. 488-496, 1991.
2. Filaretov, V. F. and Koval, E. V., "Autonomous Stabilization of Underwater Robots in the Time Manipulation Operations," Proc. Int. O.P.E.C, Osaks, Japan, pp. 382-388, 1994.
3. Goheen, K. R., "Modeling Methods for Underwater Robotic Vehicle Dynamics," J. of Robotic Systems, Vol. 8, No. 3, pp. 295-317, 1991.
4. Spangelo, L. and Egeland, O., "Generation of energy-optimal trajectories for an autonomous underwater vehicle," IEEE Int. Conf. Robotics and Automation, pp. 2107-2112, 1992.
5. Yuh, J., "Modeling and Control of Underwater Robotic Vehicles," IEEE Trans. Syst., Man. Cybern., Vol. 20, pp. 1475-1483, 1990.
6. Yoerger, D. N. and Slotine, J. E., " Robust Trajectory Control of Underwater Vehicles," IEEE J. Oceanic Eng., Vol. OE-10, pp. 463-470, 1985.
7. Wit, C. C., Diaz, E. O. and Perrier, M., "Robust Nonlinear Control of An Underwater Vehicle /Manipulator System with Composite Dynamics," IEEE Int. Conf. Robot. Automat., pp. 452-457, 1998.
8. Craig, J. J., "Introduction to Robotics, Mechanics & Control," Addison-Wesley and Sons, 1986.
9. Asada H. and Slotine J. J., "Robot Analysis and Control," John Willey and Sons, 1985.

10. Bhattacharya, R., "Dynamics of Marine Vehicles," John Willey & Sons, 1978.
11. John, J. E. A. and Haberman, W. L., "Fluid Mechanics," Prentice Hall, 1980.
12. Corless, M. and Leitmann, G., "Continuous state feedback guaranteeing uniform ultimate boundedness for uncertain dynamic systems," J. Automatic Controls, AC-26, pp. 1139-1143, 1979.

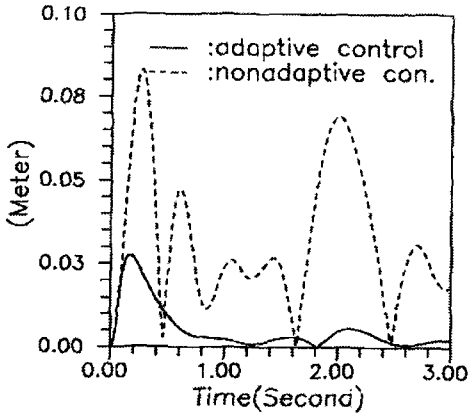

Fig. 3 Tracking errors of the trajectory

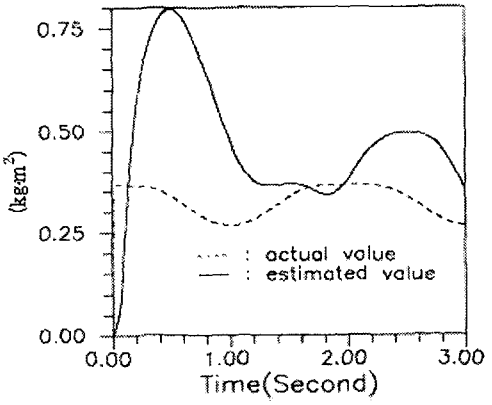

Fig. 4 Estimation of the value of a_1

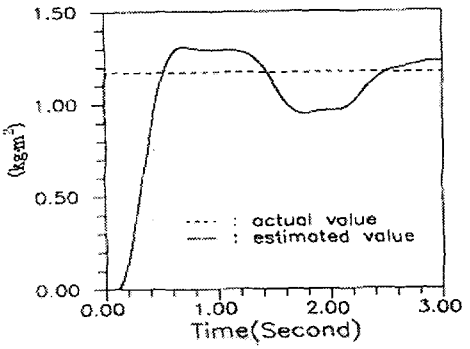

Fig. 5 Estimation of the value of a_2

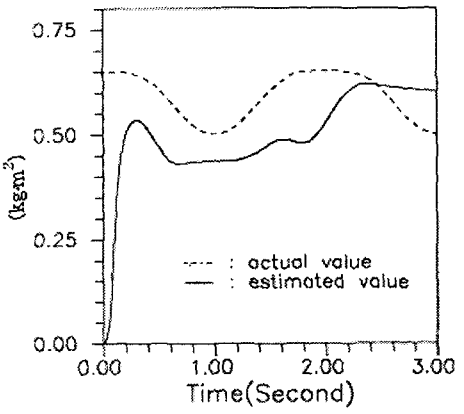

Fig. 6 Estimation of the value of a_3

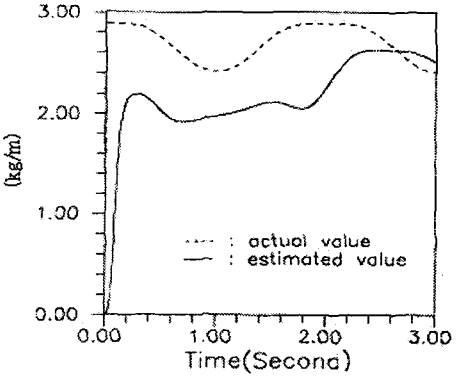

Fig. 7 Estimation of the value of b_1

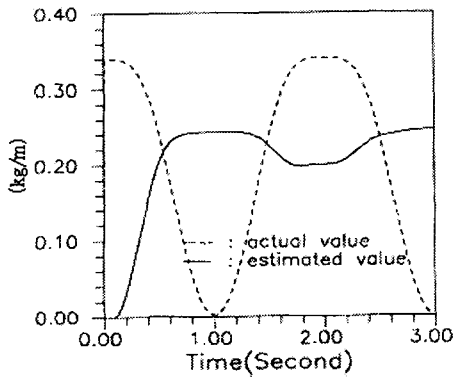

Fig. 8 Estimation of the value of b_2